

# Supplementary Material of Learning Face Deblurring Fast and Wide

Meiguang Jin  
University of Bern  
Switzerland  
jin@inf.unibe.ch

Michael Hirsch<sup>†</sup>  
Amazon Research  
Germany  
hirsch@amazon.com

Paolo Favaro  
University of Bern  
Switzerland  
favaro@inf.unibe.ch

## 1. Additional Results

In this supplementary material, we give additional results to show the robustness of our face deblurring algorithm. In the first three examples, we show the complete comparison with existing deblurring methods and in the last example we only show the comparison with the state of the art approaches. All our results are highlighted in red boxes.

## References

- [1] S. Anwar, C. Phuoc Huynh, and F. Porikli. Class-specific image deblurring. In *ICCV*, 2015. [2](#), [3](#)
- [2] A. Chakrabarti. A neural approach to blind motion deblurring. In *ECCV*, 2016. [2](#), [3](#), [4](#), [5](#)
- [3] S. Cho and S. Lee. Fast motion deblurring. *ACM Trans. Graph.*, 2009. [2](#), [3](#), [4](#)
- [4] D. Gong, J. Yang, L. Liu, Y. Zhang, I. Reid, C. Shen, A. v. d. Hengel, and Q. Shi. From motion blur to motion flow: a deep learning solution for removing heterogeneous motion blur. In *CVPR*, 2017. [2](#), [3](#), [4](#)
- [5] D. Krishnan, T. Tay, and R. Fergus. Blind deconvolution using a normalized sparsity measure. In *CVPR*, 2011. [2](#), [3](#), [4](#)
- [6] W. Lai, J. Huang, Z. Hu, N. Ahuja, and M. Yang. A comparative study for single image blind deblurring. In *CVPR*, 2016. [2](#), [3](#), [4](#)
- [7] A. Levin, Y. Weiss, F. Durand, and W. T. Freeman. Efficient marginal likelihood optimization in blind deconvolution. In *CVPR*, 2011. [2](#), [3](#), [4](#)
- [8] T. Michaeli and M. Irani. Blind deblurring using internal patch recurrence. In *ECCV*, 2014. [2](#), [3](#), [4](#)
- [9] S. Nah, T. H. Kim, and K. M. Lee. Deep multi-scale convolutional neural network for dynamic scene deblurring. In *CVPR*, 2017. [2](#), [3](#), [4](#), [5](#)
- [10] J. Pan, Z. Hu, Z. Su, and M. Yang. Deblurring face images with exemplars. In *ECCV*, 2014. [2](#), [3](#), [4](#), [5](#)
- [11] J. Pan, Z. Hu, Z. Su, and M. Yang.  $L_0$ -regularized intensity and gradient prior for deblurring text images and beyond. *IEEE TPAMI*, 2017. [2](#), [3](#), [4](#)
- [12] J. Pan, D. Sun, H. Pfister, and M.-H. Yang. Blind image deblurring using dark channel prior. In *CVPR*, 2016. [2](#), [3](#), [4](#), [5](#)
- [13] D. Perrone and P. Favaro. Total variation blind deconvolution: The devil is in the details. In *CVPR*, 2014. [2](#), [3](#), [4](#)
- [14] J. Sun, W. Cao, Z. Xu, and J. Ponce. Learning a convolutional neural network for non-uniform motion blur removal. In *CVPR*, 2015. [2](#), [3](#), [4](#)
- [15] L. Sun, S. Cho, J. Wang, and J. Hays. Edge-based blur kernel estimation using patch priors. In *ICCP*, 2013. [2](#), [3](#), [4](#)
- [16] O. Whyte, J. Sivic, A. Zisserman, and J. Ponce. Non-uniform deblurring for shaken images. *IJCV*, 2012. [2](#), [3](#), [4](#)
- [17] L. Xu and J. Jia. Two-phase kernel estimation for robust motion deblurring. In *ECCV*, 2010. [2](#), [3](#), [4](#)
- [18] L. Xu, S. Zheng, and J. Jia. Unnatural  $L_0$  sparse representation for natural image deblurring. In *CVPR*, 2013. [4](#)
- [19] H. Zhang, D. P. Wipf, and Y. Zhang. Multi-image blind deblurring using a coupled adaptive sparse prior. In *CVPR*, 2013. [2](#), [3](#), [4](#)
- [20] L. Zhong, S. Cho, D. N. Metaxas, S. Paris, and J. Wang. Handling noise in single image deblurring using directional filters. In *CVPR*, 2013. [2](#), [3](#), [4](#)

<sup>†</sup>The scientific idea and code were developed prior to joining Amazon.

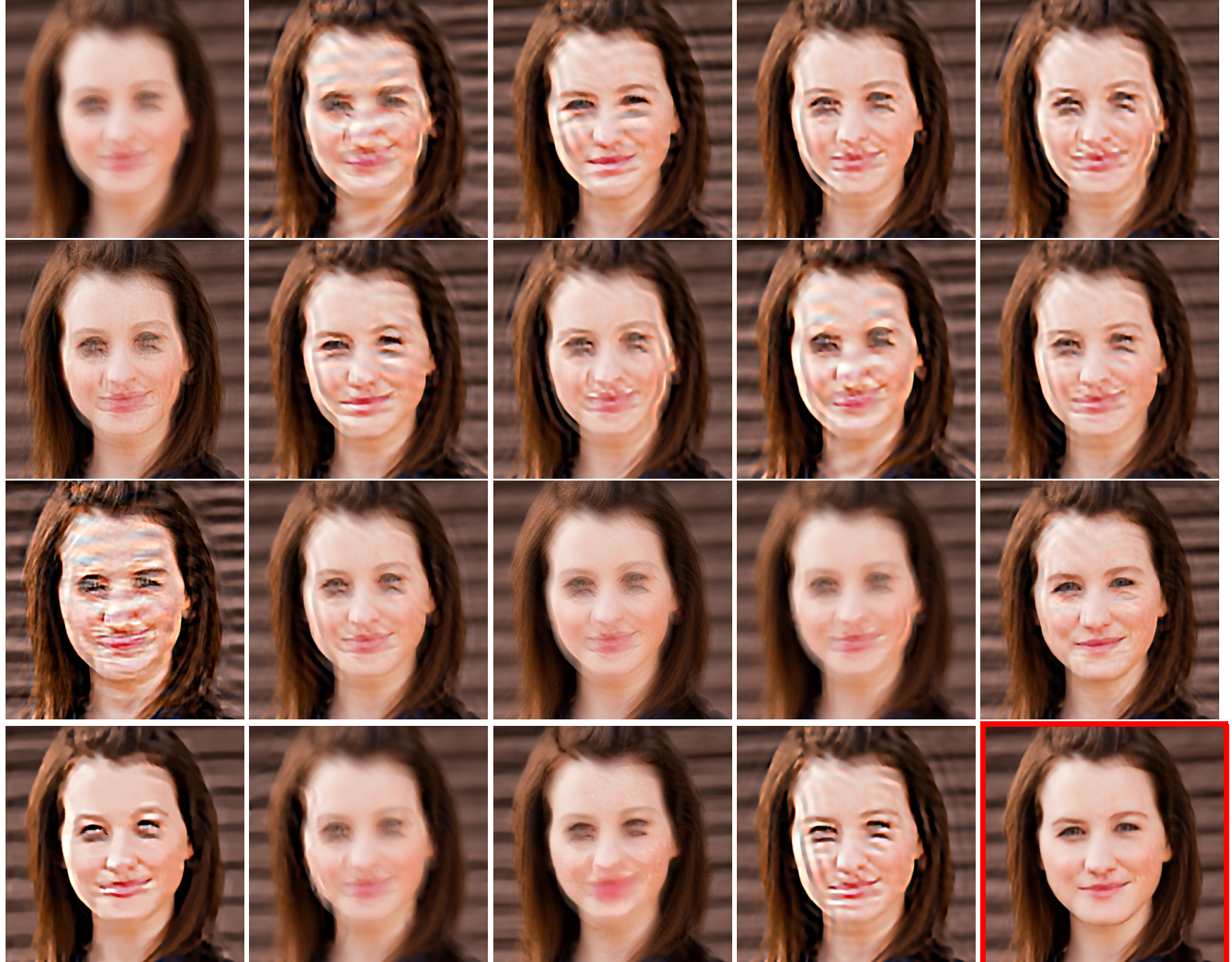


Figure 1. Visual comparisons on a synthetic blurry face image. From top to bottom and left to right images are blurry input, results of [3], [17], [5], [7], [16], [15],[19], [20], [8], [10], [13], [1], [14], [2], [12], [4], [9], [11] and ours. The blurry input is from [6].



Figure 2. Visual comparisons on a synthetic blurry face image. From top to bottom and left to right images are blurry input, results of [3], [17], [5], [7], [16], [15],[19], [20], [8], [10], [13], [1], [14], [2], [12], [4], [9], [11] and ours. The blurry input is from [6].

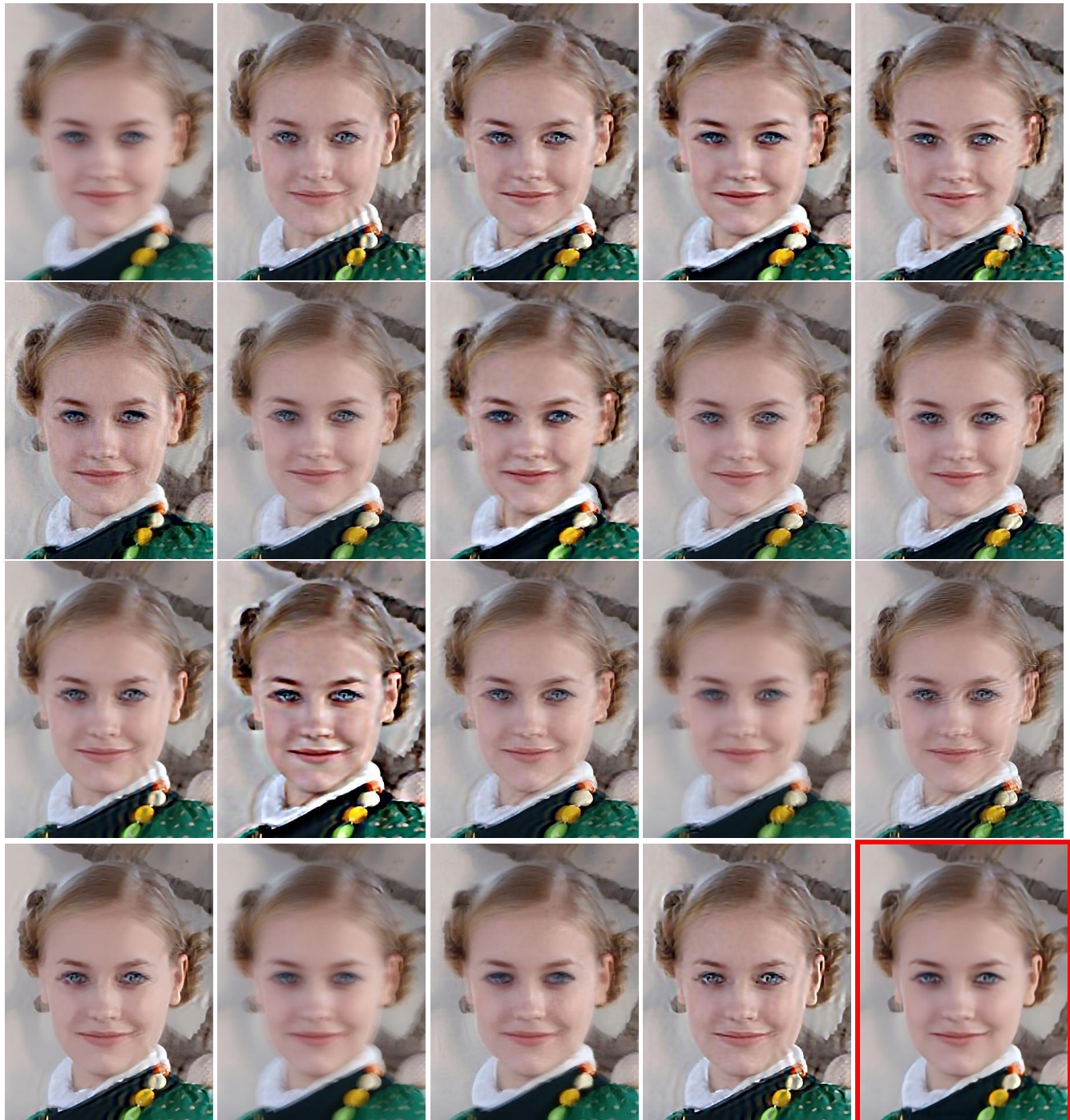


Figure 3. Visual comparisons on a real blurry face image. From top to bottom and left to right images are blurry input, results of [3], [17], [5], [7], [16], [15],[19], [20], [8], [10], [13], [18], [14], [2], [12], [4], [9], [11] and ours. The blurry input is from [6].

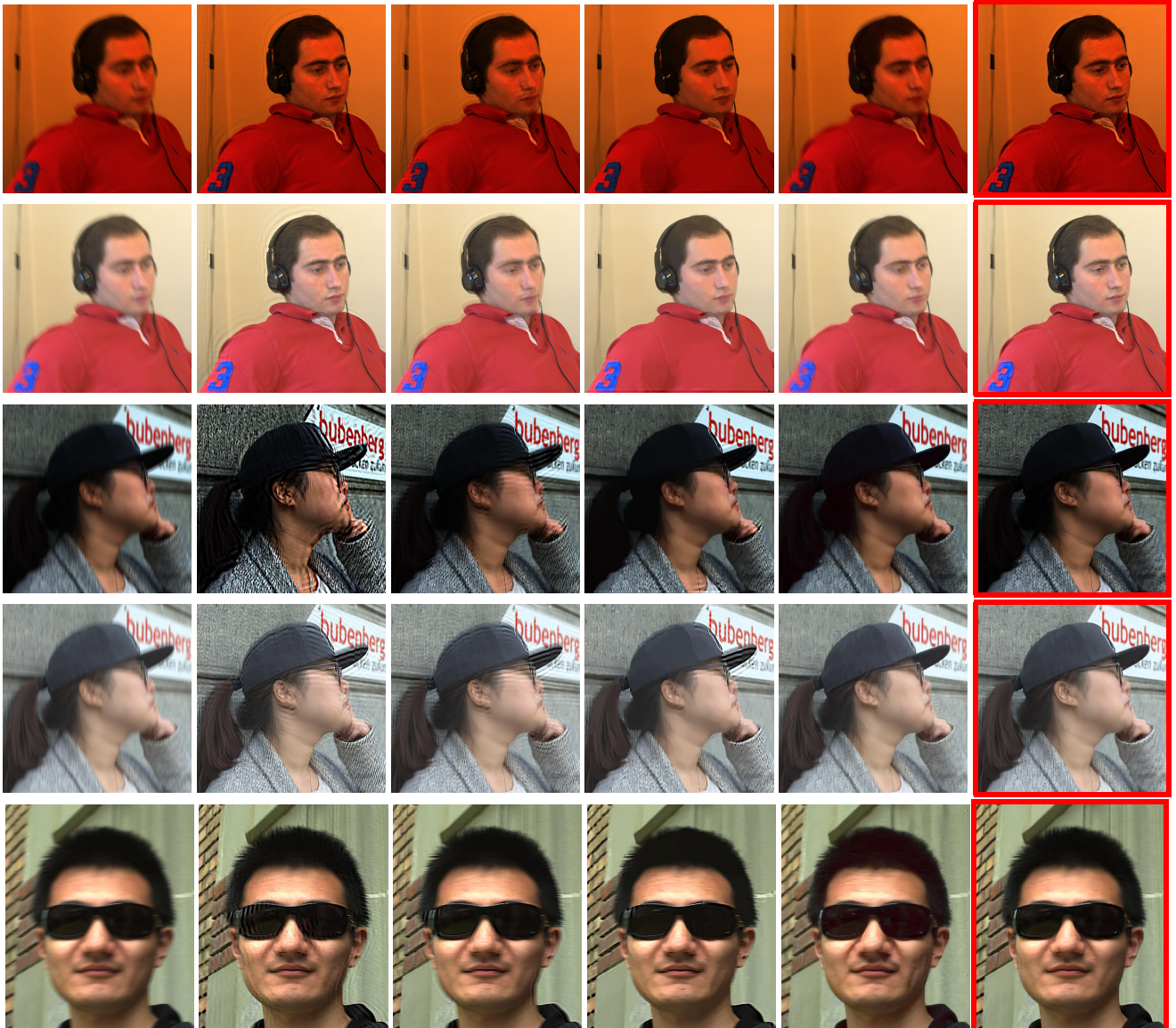


Figure 4. Visual comparisons on real face images. From left to right columns are, blurry input, results of [10], [2], [12], [9], and ours. The first and second rows are results for images w/o gamma correction, whereby a gamma of 2.2 is used. The third and fourth rows are results for images w/o gamma correction, whereby a gamma of 2.2 is used. All blurry inputs are captured with a DSLR.